ACS OMEGA

http://pubs.acs.org/journal/acsodf

Article

One-Rupee Ultrasensitive Wearable Flexible Low-Pressure Sensor

Bijender and Ashok Kumar*

Cite This: *ACS Omega* 2020, 5, 16944−16950

Read Online

ACCESS | Metrics & More | Article Recommendations

ABSTRACT: A capacitive flexible pressure sensor with polydimethylsiloxane (PDMS) as an elastomeric dielectric layer sandwiched between two flexible conducting electrodes is developed. The porosity/flexibility of PDMS has been increased by altering its microstructure by incorporating a thin layer of a scrubber into the dielectric layer to improve the pressure sensitivity. The fabricated sensor with a porous PDMS−scrubber composite (microstructured/porous PDMS layer) shows 0.058−25.84% relative capacitance change with varying static pressure from 4.4 Pa to 216 kPa. The sensor device with a porous PDMS layer showed a significantly high sensitivity (%) of 0.0083 Pa^{-1} in a low-pressure range (less than 0.022 kPa) and has a fast response, long-life, and ultralow pressure detection limit. The sensitivity associated with the device was found to vary with the effective area of the device. The pressure sensitivity associated with devices having an effective area of 324 mm^2 was 10 times more than that of the sensor having an effective area of 36 mm^2. Due to the high sensitivity of the sensor in a wide pressure range, low manufacturing cost, and simple and convenient way of fabrication, this flexible pressure sensor shows potential for pressure and wearable applications.

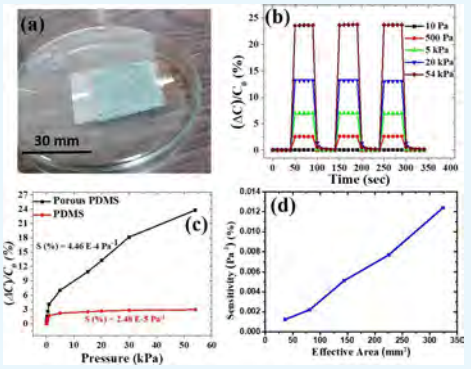

1. INTRODUCTION

Pressure sensors are highly desirable for the advancement of science and technology due to their wide applications in electronics devices, artificial intelligence, industrial production,[1−6] object detection,[7] fingerprint sensors,[8] and so forth. Based on key parameters associated with pressure sensors (sensitivity, the limit of detection, linearity, response time,[9] and reliability), we can determine their performance like the measurement accuracy and effectiveness through their sensitivity.[9] Based on sensing mechanisms, pressure sensors are mainly divided into four categories, i.e., piezoresistive,[5,10,19,20,11−18] piezocapacitive,[7,8,20−26] piezoelectric,[27−35] and triboelectric[36] pressure sensors. Among these pressure sensors, flexible pressure sensors have attracted high research interest due to their applications in wearable electronics like wearable health care monitors,[21,37−40] electronic skin applications,[41−45] medical diagnostics,[9,27,42] and human body motion monitoring[10] (vocal cord vibrations[22]). Flexible pressure sensors based on the capacitive effect, i.e., piezocapacitive flexible pressure sensors, have the main research focus due to their excellent performance, simple structure, ease of processing, and low cost. So, we focus on the piezocapacitive flexible pressure sensor, which behaves like parallel-plate capacitors having a dielectric layer sandwiched between two electrodes. The capacitance of these sensors is given by

$$C = (\varepsilon_r \cdot \varepsilon_o \cdot A)/d$$

where ε_r is the permittivity of the dielectric material, ε_o is the permittivity of the free space, A is the effective area, and d is the distance between electrodes or thickness of the dielectric layer. Capacitive-based flexible pressure sensors can detect the change in capacitance under the influence of external pressure.

Under the influence of external pressure, the thickness of the dielectric layer changes, which ultimately leads to a change in capacitance of the sensor. Moreover, as the effective area of the pressure sensor increases, a large variation in capacitance can be observed. Piezocapacitive flexible pressure sensors mainly consist of top/bottom flexible conducting electrodes and an elastomeric dielectric layer.[24,25] For flexible conducting electrodes of capacitive pressure sensors, indium tin oxide (ITO) coated with poly(ethylene terephthalate) (PET) substrates is the best choice because the PET film transfers most of the stress when pressure is applied, so there is no damage to the ITO layer, and a uniform pressure is applied all over the device due to PET. For the elastomeric dielectric layer, polydimethylsiloxane (PDMS) is a promising candidate among various elastomers due to its excellent flexibility and elasticity, and the main advantage is that we can modify the

Received: May 15, 2020
Accepted: June 9, 2020
Published: June 29, 2020

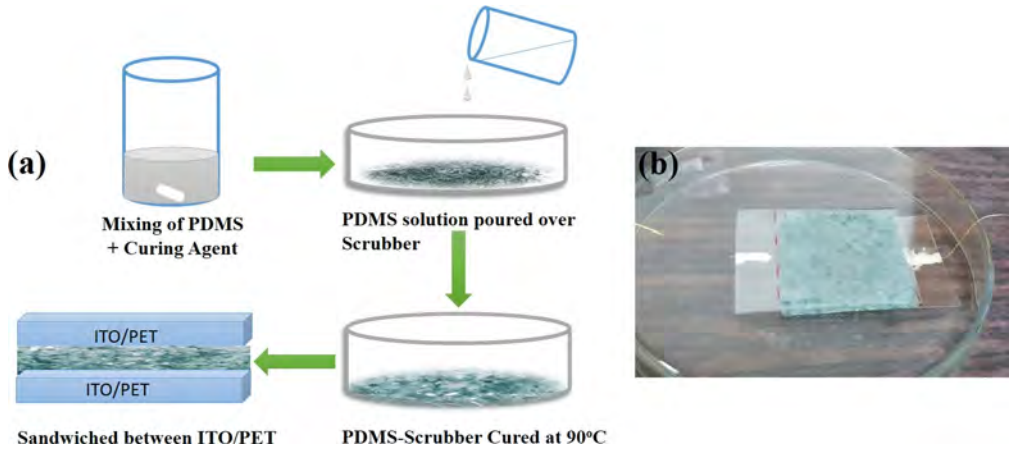

Figure 1. (a) Schematic diagram of the fabrication of the capacitive pressure sensor with a porous PDMS dielectric layer (b) Real image of the fabricated sensor in which the porous PDMS (PDMS−scrubber) layer is sandwiched between ITO-coated PET substrates.

structure of PDMS as per the requirement of the application. Many researchers reported that the pressure sensitivity coefficients could be improved by modifying the elastomer dielectric layer and formation of the PDMS elastomer either by making it porous[21,46] or by introducing bubbles into it[47] or by making a wrinkled microstructure[26] of the PDMS layer. So, all we need is a low manufacturing cost, low energy-consuming, and simple-structured flexible pressure sensor with high sensitivity applicable for wearable sensing devices.

In this work, we developed a low-cost capacitive-based flexible pressure sensor with a porous PDMS layer. The porosity of the PDMS film was improved by altering its microstructure by incorporating a thin layer of a scrubber into the dielectric layer. The performance of the PDMS−scrubber composite sensor has been described in this article over a wide range of pressure. The effect of the effective area of the sensor on the sensitivity of the pressure sensor is also studied. The fabricated sensor showed a high sensitivity and linear response, which makes it suitable as an ultrasensitive, flexible pressure sensor for biological and medical applications and ultrahigh sensitivity transfer pressure standards.

2. RESULTS AND DISCUSSION

The detailed process of fabrication of the flexible pressure sensor is illustrated in Figure 1. First, the dielectric layer was prepared by using the PDMS−scrubber composite as shown in Figure 1a, and Figure 1b shows the photo of the pressure sensor in which a dielectric layer was sandwiched between flexible electrodes. The detailed process of fabricating the dielectric layer and flexible pressure sensor is described in the Experimental Section.

Figure 2a shows the cross-sectional SEM image of the cured PDMS layer only (unstructured PDMS layer), which has no porosity inside it, whereas from Figure 2b, which is the cross-sectional SEM image of the PDMS−scrubber composite, it can be seen that there is a porosity present in the form of bubbles. Similarly, Figure 2c,d represents the microscopic images of the scrubber and PDMS−scrubber composite, respectively, in which Figure 2d again shows the porosity in the PDMS layer in the form of bubbles, voids, and air traps.

The pressure-dependent measurement of capacitance was performed by putting external pressure on the sensor simply by putting dead weights on a thin glass slide, as discussed in

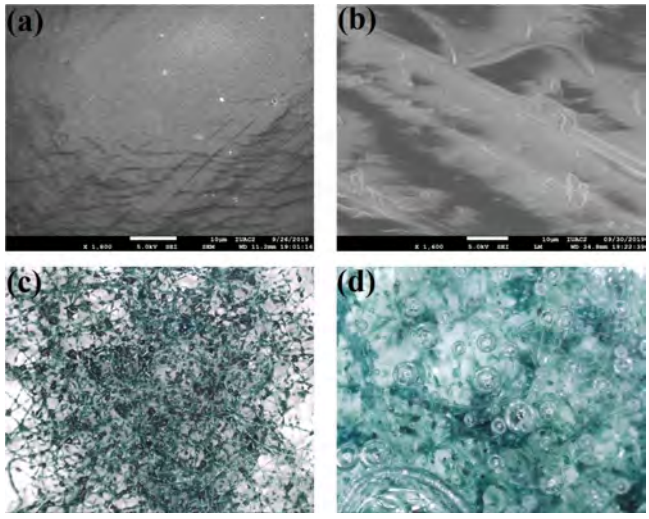

Figure 2. (a) Cross-sectional SEM images of the PDMS layer indicate that there was no porosity present. (b) Cross-sectional SEM image of the fabricated porous elastomeric dielectric layer, which indicates the presence of porosity. (c) Microscopic image of the scrubber. (d) Microscopic images of the PDMS−scrubber (porous PDMS) film, which are taken with the help of a digital microscope.

Section 4.3, which is kept on a fabricated pressure sensor. The pressure is defined as

$$P = \frac{F}{A} \text{or} \frac{mg}{A}$$

where m is the mass, g is the acceleration due to gravity, and A is the effective area on which the load is applied. We fixed the effective area (A) by putting a glass slide of a defined area on the sensor; as a result, the pressure was changed only by changing the values of mass. The dead weights for applying different pressures were made according to the glass slide having a size of 12 mm × 12 mm (area = 144 mm^2). The capacitance (C) with varying weights/pressures was measured, and then pressure sensitivity (S) of the pressure sensor was calculated. The variation in capacitance (C) was measured as a function of time at 1 MHz with varying applied pressure in the range of 10 Pa−54 kPa by loading and unloading weights on the sensor devices having porous and unstructured PDMS

https://dx.doi.org/10.1021/acsomega.0c02278
ACS Omega 2020, 5, 16944−16950

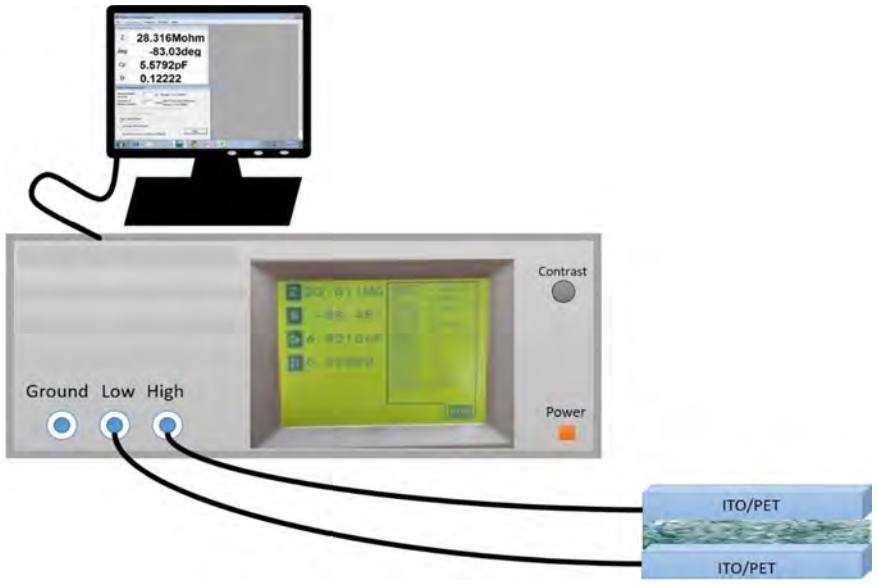

Figure 3. Schematic diagram of the experimental setup for measuring the relative change in capacitance concerning different applied pressures for the fabricated device (as shown in Figure 1).

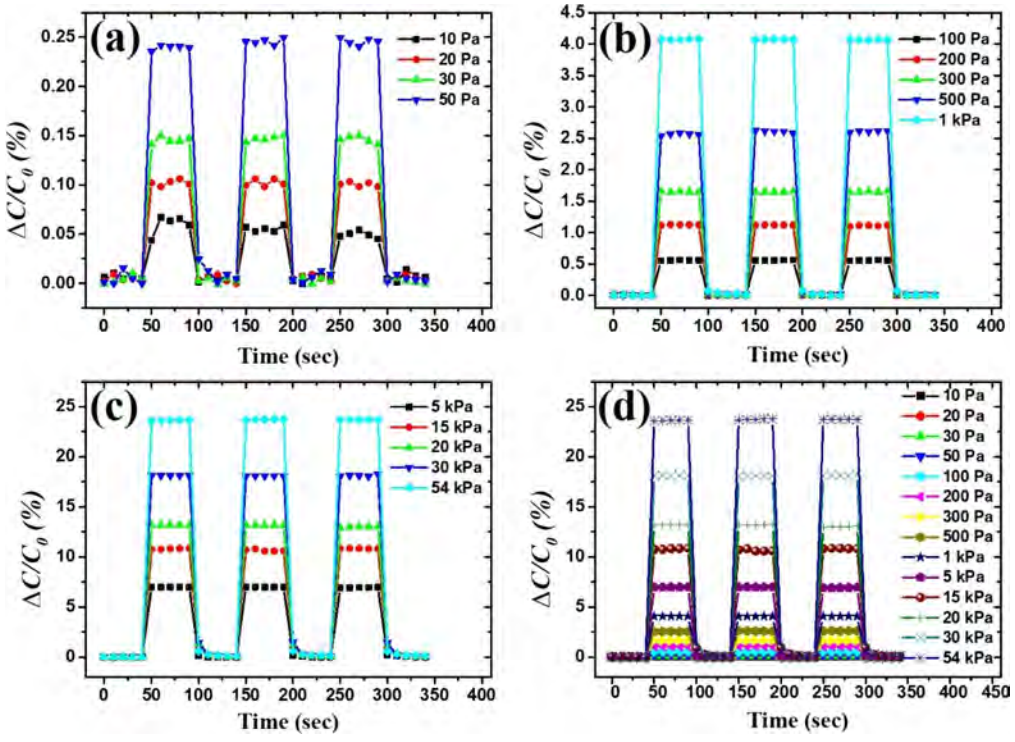

Figure 4. Variation of relative changes in capacitance as a function of time at different applied pressure ranges of (a) 10−50 Pa. (b) 100 Pa−1 kPa. (c) 5− 54 kPa, and (d) 10 Pa−54 kPa.

layers. The schematic diagram of the experimental setup for measuring the variation of capacitance is shown in Figure 3.

The relative change in capacitance ($\Delta C/C_0$) with time at different pressures ranging from 10 Pa to 54 kPa is shown in Figure 4, where $\Delta C = C - C_0$, and C_0 is the value of capacitance of the device without the application of loads/dead weights. The value of C_0 changes with the change in the dimension of glass slides and weights.

The pressure sensor having a porous PDMS layer shows 0.06% relative change in capacitance. It can detect a pressure of 10 Pa for an effective area of 144 mm^2, while the device having only a PDMS layer has shown only 0.03% relative change in capacitance for a pressure of 10 Pa. As the applied pressure was increased, the relative change in capacitance was also increased as shown in Figure 4, and the maximum value of $\Delta C/C_0$ was obtained as 23.76% for 54 kPa, as shown in Table 1, which is nearly 10 times greater than the device with only the PDMS layer (only 2.96% change in capacitance) as shown in Figure 6a.

For sensing characteristics, a graph was plotted between $\Delta C/C_0$ (%) and varying applied pressure (P) in the range of 10 Pa−54 kPa (shown in Figure 5a). The slope of the graph gives

https://dx.doi.org/10.1021/acsomega.0c02278
ACS Omega 2020, 5, 16944−16950

Table 1. Relative Change in Capacitance (%) are Shown with Varying Pressure for Given Effective Area Values from 36 to 324 mm^2

s. no.	pressure (Pa), 36 mm^2	$\Delta C/C_O$ (%)	pressure (Pa), 81 mm^2	$\Delta C/C_O$ (%)	pressure (Pa), 144 mm^2	$\Delta C/C_O$ (%)	pressure (Pa), 225 mm^2	$\Delta C/C_O$ (%)	pressure (Pa), 324 mm^2	$\Delta C/C_O$ (%)
1	40	0.048	17.857	0.048	10	0.067	6.4102	0.048	4.444	0.058
2	80	0.088	35.714	0.080	20	0.106	12.82	0.079	8.888	0.089
3	120	0.127	53.571	0.124	30	0.15	19.23	0.105	13.333	0.124
4	200	0.191	89.285	0.223	50	0.249	32.051	0.157	22.222	0.204
5	400	0.475	178.571	0.555	100	0.565	64.102	0.511	44.444	0.502
6	800	0.989	357.142	1.049	200	1.125	128.205	0.946	88.888	1.069
7	1200	1.512	535.714	1.471	300	1.65	192.307	1.43	133.333	1.585
8	2000	2.446	892.857	2.156	500	2.621	320.512	2.468	222.222	2.711
9	4000	4.113	1785.714	4.354	1000	4.081	641.025	3.922	444.444	4.227
10	20,000	7.628	8928.571	8.324	5000	6.994	3205.12	7.901	2222.222	8.031
11	60,000	11.215	26,785.71	12.505	15,000	10.874	9615.38	11.631	6666.667	12.745
12	80,000	13.445	35,714.29	14.925	20,000	13.209	12,820.51	13.868	8888.889	15.576
13	120,000	17.964	53,571.43	20.003	30,000	18.112	19,230.77	18.351	13,333.33	21.169
14	216,000	25.84	96,428.57	22.599	54,000	23.764	34,615.38	24.603	24,000	25.337

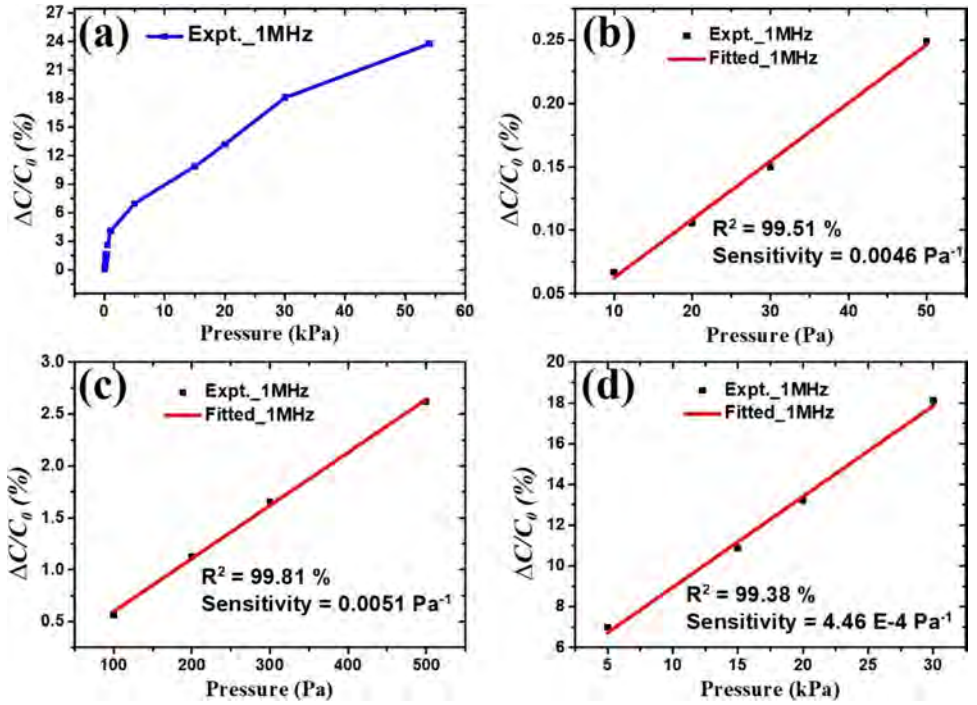

Figure 5. Variation of capacitance change ($\Delta C/C_0$) as a function of the applied pressure ranges (a) 10 Pa−54 kPa, (b) 10−50 Pa, (c) 100−500 Pa, and (d) 5−30 kPa.

the value of sensitivity (S), which is defined as $S = \delta(\Delta C/C_0)/\delta_p$, where δ ($\Delta C/C_0$) is the change in the value of relative change in capacitance, and δ_p is the change in the value of applied pressure.[21] The curve is shown in Figure 5a and is divided into three different regions where the first region is the low-pressure range (10 Pa $\leq P \leq$ 50 Pa), the second region is the medium-pressure range (100 Pa $\leq P \leq$ 1000 Pa), and the third region is the high-pressure range (5 kPa $\leq P \leq$ 54 kPa). The sensor of the porous PDMS layer showed a linear response in low-, medium-, and high-pressure ranges having the sensitivities S (%) of 0.0046 (Figure 5b), 0.0051 (Figure 5c), and 4.46 × 10^{-4} Pa^{-1} (Figure 5d), respectively.

The device with a pure PDMS layer has 0.03% relative change in capacitance for the pressure of 10 Pa and 2.96% for 54 kPa as shown in Figure 6a, whereas the device of a porous PDMS layer shows 0.06% for 10 Pa and 23.76% relative change in capacitance for 54 kPa pressure. The variation in the relative change in the capacitance as a function of pressure for only PDMS as a dielectric layer is shown in Figure 6b. The sensor device with a porous PDMS layer showed significantly high sensitivity in low- and high-pressure ranges as compared to the device of only a PDMS layer (Figure 6c).

Four more glass slides having areas of 36, 81, 225, and 324 mm^2 were taken to study the variation of capacitance with varying effective areas of the sensor, and the same measurements were also performed as it was done for the slide having an area of 144 mm^2. Since the pressure is inversely proportional to the effective area, the pressure decreases with an increase in the effective area. The values of relative change in capacitance with varying pressure for given effective areas of the device are shown in Table 1.

https://dx.doi.org/10.1021/acsomega.0c02278
ACS Omega 2020, 5, 16944−16950

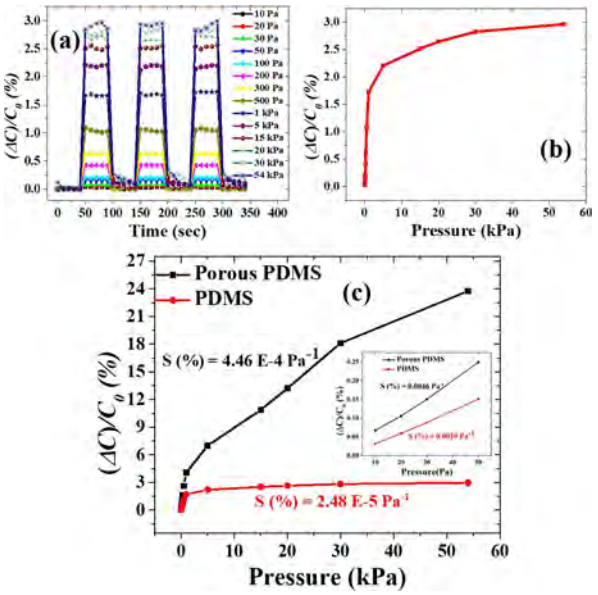

Figure 6. Variation of relative change in capacitance of only PDMS (a) as a function of time at different applied pressures, (b) as a function of an applied pressure range of 10 Pa−54 kPa, and (c) as a function of applied pressure having microstructured (porous PDMS) and unstructured PDMS layers (inset shows the low-pressure range of 10−50 Pa).

Hence, the value of sensitivities was calculated according to the pressure ranges: low-pressure range (4−200 Pa), medium-pressure range (44−2000 Pa), and high-pressure range (2.2−120 kPa) as it was done for the 144 mm^2 effective area. The sensitivity (%) with varying effective areas of the device was plotted for low-pressure, medium-pressure, and high-pressure regions and shown in Figure 7a−c, respectively.

From Figure 7, it was observed that the pressure sensitivity of the device increased by increasing the effective area. The sensitivity of the pressure sensor with an effective area of 324 mm^2 was approximately 10 times better in low-, medium-, and high-pressure regions than that of the pressure sensor with an effective area of 36 mm^2. The value of sensitivity of the device for different pressure regions with varying effective areas is also shown in Table 2. The $\Delta C/C_0$ values for different pressure regions were also measured at 1 kHz, and it was concluded that the fabricated flexible pressure sensor could not detect the pressure lower than 50 Pa, but it can detect 10 Pa pressure at 1 MHz frequency. In future studies, we will explore its suitability as a pressure sensor in biological applications.

Table 2. Variation of Sensitivity (%) for Different Effective Areas of the Developed Pressure Sensor in Low-, Medium-, and High-Pressure Regions

pressure range	low (4−200 Pa)	medium (44−2000 Pa)	high (2.2−120 kPa)
effective area (mm^2)	sensitivity (%) (Pa^{-1})	sensitivity (%) (Pa^{-1})	sensitivity (%) (Pa^{-1})
36	0.0009	0.0012	1.04×10^{-4}
81	0.0025	0.0022	2.62×10^{-4}
144	0.0046	0.0051	4.46×10^{-4}
225	0.0053	0.0077	6.54×10^{-4}
324	0.0083	0.0124	0.0012

3. CONCLUSIONS

A low-cost capacitive flexible ultrahigh sensitive pressure sensor was developed, which shows a quick response for repeated loading/unloading of external pressure. This pressure sensor having a porous PDMS−scrubber composite as an active dielectric layer showed a largely improved sensitivity (%) of 0.0046 Pa^{-1} in the low-pressure region, 0.0051 Pa^{-1} in the medium-pressure region, and 4.46×10^{-4} Pa^{-1} in the high-pressure region for an effective area of 144 mm^2 as compared to the device of only the PDMS layer. The pressure sensitivity of the sensor increased with an increase in the effective area of the device. As the effective area of the fabricated pressure sensor was changed from 36 to 324 mm^2, the pressure sensitivity associated with the sensing device was 10 times enhanced, and the device with an effective area of 324 mm^2 has an ultralow detection limit (less than 5 Pa) due to its high sensitivity in the low-pressure range. Nearly one-rupee cost and high sensitivity of the fabricated flexible sensor in the full pressure range up to 216 kPa showed potential for reference pressure standards and biological applications.

4. EXPERIMENTAL DETAILS

4.1. Fabrication of the Dielectric Layer. Polydimethylsiloxane (PDMS), a prepolymer, and its curing agent (Dow Corning, Sylgard 184) were taken in a weight ratio of 10:1 and mixed them with the help of a magnetic stirrer at a rate of 1000 rpm for 2 h. The Household Scotch Brite scrubber pad of 3 M India Company was purchased, and a thin layer of the scrubber from the scrubber pad was peeled off and placed in a Petri dish. After that, PDMS solution was poured over the thin layer of

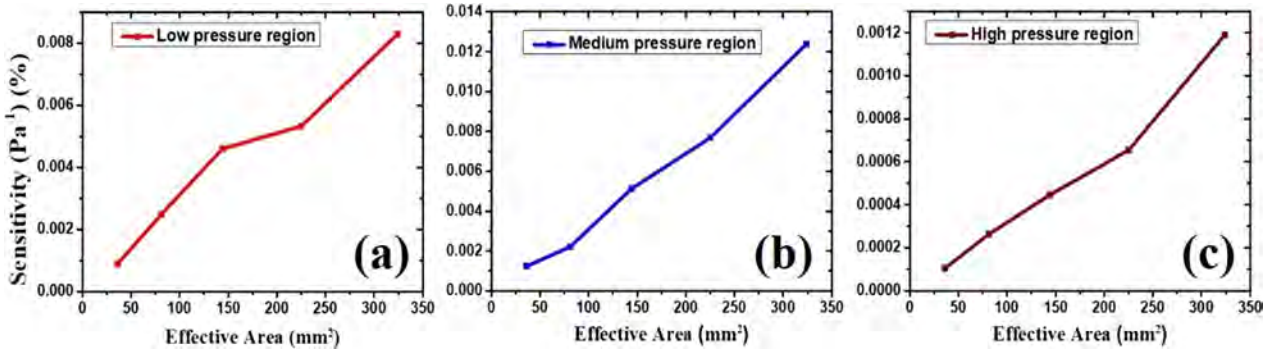

Figure 7. Variation of sensitivity (%) as a function of the effective area for the (a) low-pressure range (4−200 Pa), (b) medium-pressure range (44−2000 Pa), and (c) high-pressure range (2.2−120 kPa).

https://dx.doi.org/10.1021/acsomega.0c02278
ACS Omega 2020, 5, 16944−16950

the scrubber for the cross-linking and annealed it at 90° C for 12 h (shown in Figure 1a). An annealed porous PDMS−scrubber composite film having dimensions of 30 mm × 30 mm and thickness of nearly 3 mm was used as a dielectric layer in our capacitive-type pressure sensor.

4.2. Fabrication of the Pressure Sensor. For the formation of the capacitor-based device, the fabricated dielectric layer of the porous PDMS−scrubber composite was sandwiched between ITO-coated PET substrates with a thickness of 130 μm (shown in Figure 1a), which behave as top and bottom electrodes. For the adhesion between electrodes and the dielectric layer, a very thin layer of PDMS solution was used over the substrates, and then for the strong adhesion, it was annealed at 90 °C. For electrical contacts, a copper wire was attached to both the electrode substrates with the help of silver paint, as shown in Figure 1b.

4.3. Characterization and Measurements. The porosity of the fabricated sample was identified from a cross-sectional image with the help of a scanning electron microscopy (SEM) technique, and optical images were also captured by a digital microscope (Celestron handheld digital microscope). Thin glass slides were used for varying effective areas having the dimensions of 6 mm × 6 mm (area = 36 mm^2) of 150 mg weight, 9 mm × 9 mm (area = 81 mm^2) of 264 mg weight, 12 mm × 12 mm (area = 144 mm^2) of 554 mg weight, 15 mm × 15 mm (area = 225 mm^2) of 764 mg weight, and 18 mm × 18 mm (area = 324 mm^2) of 1140 mg weight; and the fabricated device area (900 mm^2) is greater than that of the glass slides used for controlling the effective area. The static pressure was applied to the thin glass slide kept on the fabricated device by using different dead weights having dimensions less than the glass slides for homogeneous application of applied loads.

The capacitance of the fabricated pressure sensor was measured over the range of 1 kHz−1 MHz; however, the 1 MHz frequency was used for all the capacitive measurements for possible miniaturization of the device and conversion of output capacitance as a digital display unit. The variation of capacitance of the pressure sensor having only PDMS as the dielectric layer was also measured at room temperature using an LCR meter (HIOKI 3532−50 LCR Hi-TESTER). We have taken adequate precautions during the measurement: (1) the sensing devices were kept on a rock-solid insulating surface/table so that device should get perfect deformation (change in capacitance) under applied loads, and (2) loading and unloading of weights on the sensor device were positioned at the middle of the glass slide without disturbing the device.

AUTHOR INFORMATION

Corresponding Author

Ashok Kumar − *CSIR-National Physical Laboratory, New Delhi 110012, India; Academy of Scientific and Innovative Research (AcSIR), CSIR-National Physical Laboratory (CSIR-NPL) Campus, New Delhi 110012, India*; Email: ashok553@nplindia.org

Author

Bijender − *CSIR-National Physical Laboratory, New Delhi 110012, India; Academy of Scientific and Innovative Research (AcSIR), CSIR-National Physical Laboratory (CSIR-NPL) Campus, New Delhi 110012, India*; orcid.org/0000-0002-5104-7170

Complete contact information is available at: https://pubs.acs.org/10.1021/acsomega.0c02278

Notes

The authors declare no competing financial interest.

ACKNOWLEDGMENTS

The authors would like to thank the director of CSIR-NPL and head of the Physico-Mechanical Metrology division, CSIR-NPL, for their support and constant encouragement. We also want to thank the CSIR-NPL for partial funding for pursuing the project. Mr. Bijender thanks AcSIR for pursuing a Ph.D. program and CSIR for financial support. The authors also want to thank Mr. Charanjeet Singh and Mr. Shubham Kumar for their constant help and support.

REFERENCES

(1) Chang, W.-Y.; Chen, C.-C.; Chang, C.-C.; Yang, C.-L. An Enhanced Sensing Application Based on a Flexible Projected Capacitive-Sensing Mattress. *Sensors* **2014**, *14*, 6922−6937.

(2) Chang, W.-Y.; Fang, T.-H.; Yeh, S.-H.; Lin, Y.-C. Flexible Electronics Sensors for Tactile Multi-Touching. *Sensors* **2009**, *9*, 1188−1203.

(3) Jung, S.; Kim, J. H.; Kim, J.; Choi, S.; Lee, J.; Park, I.; Hyeon, T.; Kim, D.-H. Reverse-Micelle-Induced Porous Pressure-Sensitive Rubber for Wearable Human-Machine Interfaces. *Adv. Mater.* **2014**, *26*, 4825−4830.

(4) Kang, A.; Lin, J.; Ji, X.; Wang, W.; Li, H.; Zhang, C.; Han, T. A High-Sensitivity Pressure Sensor Based on Surface Transverse Wave. *Sens. Actuators, A* **2012**, *187*, 141−146.

(5) Pang, C.; Lee, G.-Y.; Kim, T.-i.; Kim, S. M.; Kim, H. N.; Ahn, S.-H.; Suh, K.-Y. A Flexible and Highly Sensitive Strain-Gauge Sensor Using Reversible Interlocking of Nanofibres. *Nat. Mater.* **2012**, *11*, 795−801.

(6) Jiang, C.; Markutsya, S.; Pikus, Y.; Tsukruk, V. V. Freely Suspended Nanocomposite Membranes as Highly Sensitive Sensors. *Nat. Mater.* **2004**, *3*, 721−728.

(7) Metzger, C.; Fleisch, E.; Meyer, J.; Dansachmüller, M.; Graz, I.; Kaltenbrunner, M.; Keplinger, C.; Schwödiauer, R.; Bauer, S. Flexible-Foam-Based Capacitive Sensor Arrays for Object Detection at Low Cost. *Appl. Phys. Lett.* **2008**, *92*, No. 013506.

(8) Sato, N.; Shigematsu, S.; Morimura, H.; Yano, M.; Kudou, K.; Kamei, T.; Machida, K. Novel Surface Structure and Its Fabrication Process for MEMS Fingerprint Sensor. *IEEE Trans. Electron Devices* **2005**, *52*, 1026−1032.

(9) Zang, Y.; Zhang, F.; Di, C. a.; Zhu, D. Advances of Flexible Pressure Sensors toward Artificial Intelligence and Health Care Applications. *Mater. Horiz.* **2015**, *2*, 140−156.

(10) Liu, Q.; Chen, J.; Li, Y.; Shi, G. High-Performance Strain Sensors with Fish-Scale-Like Graphene-Sensing Layers for Full-Range Detection of Human Motions. *ACS Nano* **2016**, *10*, 7901−7906.

(11) Lou, Z.; Chen, S.; Wang, L.; Jiang, K.; Shen, G. An Ultra-Sensitive and Rapid Response Speed Graphene Pressure Sensors for Electronic Skin and Health Monitoring. *Nano Energy* **2016**, *23*, 7−14.

(12) Garain, S.; Jana, S.; Sinha, T. K.; Mandal, D. Design of In Situ Poled Ce^{3+} −Doped Electrospun PVDF/Graphene Composite Nanofibers for Fabrication of Nanopressure Sensor and Ultrasensitive Acoustic Nanogenerator. *ACS Appl. Mater. Interfaces* **2016**, *8*, 4532−4540.

(13) Tai, Y.; Lubineau, G. Smart Threads: Double-Twisted Conductive Smart Threads Comprising a Homogeneously and a Gradient-Coated Thread for Multidimensional Flexible Pressure-Sensing Devices (Adv. Funct. Mater. 23/2016). *Adv. Funct. Mater.* **2016**, *26*, 4037.

(14) Song, X.; Sun, T.; Yang, J.; Yu, L.; Wei, D.; Fang, L.; Lu, B.; Du, C.; Wei, D. Direct Growth of Graphene Films on 3D Grating Structural Quartz Substrates for High-Performance Pressure-Sensitive Sensors. *ACS Appl. Mater. Interfaces* **2016**, *8*, 16869−16875.

(15) Liu, X.; Zhu, Y.; Nomani, M. W.; Wen, X.; Hsia, T.-Y.; Koley, G. A Highly Sensitive Pressure Sensor Using a Au-Patterned

Polydimethylsiloxane Membrane for Biosensing Applications. *J. Micromech. Microeng.* **2013**, *23*, No. 025022.
(16) Choong, C.-L.; Shim, M.-B.; Lee, B.-S.; Jeon, S.; Ko, D.-S.; Kang, T.-H.; Bae, J.; Lee, S. H.; Byun, K.-E.; Im, J.; Jeong, Y. J.; Park, C. E.; Park, J.-J.; Chung, U.-I. Highly Stretchable Resistive Pressure Sensors Using a Conductive Elastomeric Composite on a Micropyramid Array. *Adv. Mater.* **2014**, *26*, 3451−3458.
(17) Burg, B. R.; Helbling, T.; Hierold, C.; Poulikakos, D. Piezoresistive Pressure Sensors with Parallel Integration of Individual Single-Walled Carbon Nanotubes. *J. Appl. Phys.* **2011**, *109*, No. 064310.
(18) Azhari, S.; Yousefi, A. T.; Tanaka, H.; Khajeh, A.; Kuredemus, N.; Bigdeli, M. M.; Hamidon, M. N. Fabrication of Piezoresistive Based Pressure Sensor via Purified and Functionalized CNTs/PDMS Nanocomposite: Toward Development of Haptic Sensors. *Sens. Actuators, A* **2017**, *266*, 158−165.
(19) Sepúlveda, A. T.; Guzman de Villoria, R.; Viana, J. C.; Pontes, A. J.; Wardle, B. L.; Rocha, L. A. Full Elastic Constitutive Relation of Non-Isotropic Aligned-CNT/PDMS Flexible Nanocomposites. *Nanoscale* **2013**, *5*, 4847−4854.
(20) Lipomi, D. J.; Vosgueritchian, M.; Tee, B. C.-K.; Hellstrom, S. L.; Lee, J. A.; Fox, C. H.; Bao, Z. Skin-like Pressure and Strain Sensors Based on Transparent Elastic Films of Carbon Nanotubes. *Nat. Nanotechnol.* **2011**, *6*, 788−792.
(21) Chen, S.; Zhuo, B.; Guo, X. Large Area One-Step Facile Processing of Microstructured Elastomeric Dielectric Film for High Sensitivity and Durable Sensing over Wide Pressure Range. *ACS Appl. Mater. Interfaces* **2016**, *8*, 20364−20370.
(22) Shuai, X.; Zhu, P.; Zeng, W.; Hu, Y.; Liang, X.; Zhang, Y.; Sun, R.; Wong, C.-P. Highly Sensitive Flexible Pressure Sensor Based on Silver Nanowires-Embedded Polydimethylsiloxane Electrode with Microarray Structure. *ACS Appl. Mater. Interfaces* **2017**, *9*, 26314−26324.
(23) You, B.; Han, C. J.; Kim, Y.; Ju, B.-K.; Kim, J.-W. A Wearable Piezocapacitive Pressure Sensor with a Single Layer of Silver Nanowire-Based Elastomeric Composite Electrodes. *J. Mater. Chem. A* **2016**, *4*, 10435−10443.
(24) Lee, J.; Kwon, H.; Seo, J.; Shin, S.; Koo, J. H.; Pang, C.; Son, S.; Kim, J. H.; Jang, Y. H.; Kim, D. E.; Lee, T. Conductive Fiber-Based Ultrasensitive Textile Pressure Sensor for Wearable Electronics. *Adv. Mater.* **2015**, *27*, 2433−2439.
(25) Joo, Y.; Byun, J.; Seong, N.; Ha, J.; Kim, H.; Kim, S.; Kim, T.; Im, H.; Kim, D.; Hong, Y. Silver Nanowire-Embedded PDMS with a Multiscale Structure for a Highly Sensitive and Robust Flexible Pressure Sensor. *Nanoscale* **2015**, *7*, 6208−6215.
(26) Baek, S.; Jang, H.; Kim, S. Y.; Jeong, H.; Han, S.; Jang, Y.; Kim, D. H.; Lee, H. S. Flexible Piezocapacitive Sensors Based on Wrinkled Microstructures: Toward Low-Cost Fabrication of Pressure Sensors over Large Areas. *RSC Adv.* **2017**, *7*, 39420−39426.
(27) Dagdeviren, C.; Su, Y.; Joe, P.; Yona, R.; Liu, Y.; Kim, Y. S.; Huang, Y.; Damadoran, A. R.; Xia, J.; Martin, L. W.; Huang, Y.; Rogers, J. A. Conformable Amplified Lead Zirconate Titanate Sensors with Enhanced Piezoelectric Response for Cutaneous Pressure Monitoring. *Nat. Commun.* **2014**, *5*, 4496.
(28) Chun, J.; Lee, K. Y.; Kang, C.-Y.; Kim, M. W.; Kim, S.-W.; Baik, J. M. Embossed Hollow Hemisphere-Based Piezoelectric Nanogenerator and Highly Responsive Pressure Sensor. *Adv. Funct. Mater.* **2014**, *24*, 2038−2043.
(29) Pan, C.; Dong, L.; Zhu, G.; Niu, S.; Yu, R.; Yang, Q.; Liu, Y.; Wang, Z. L. High-Resolution Electroluminescent Imaging of Pressure Distribution Using a Piezoelectric Nanowire LED Array. *Nat. Photonics* **2013**, *7*, 752−758.
(30) Persano, L.; Dagdeviren, C.; Su, Y.; Zhang, Y.; Girardo, S.; Pisignano, D.; Huang, Y.; Rogers, J. A. High Performance Piezoelectric Devices Based on Aligned Arrays of Nanofibers of Poly(Vinylidenefluoride-Co-Trifluoroethylene). *Nat. Commun.* **2013**, *4*, 1633.
(31) Lee, J.-H.; Yoon, H.-J.; Kim, T. Y.; Gupta, M. K.; Lee, J. H.; Seung, W.; Ryu, H.; Kim, S.-W. Micropatterned P(VDF-TrFE) Film-Based Piezoelectric Nanogenerators for Highly Sensitive Self-Powered Pressure Sensors. *Adv. Funct. Mater.* **2015**, *25*, 3203−3209.
(32) Choi, W.; Lee, J.; Yoo, Y. K.; Kang, S.; Kim, J.; Lee, J. H. Enhanced Sensitivity of Piezoelectric Pressure Sensor with Microstructured Polydimethylsiloxane Layer. *Appl. Phys. Lett.* **2014**, *104*, 123701.
(33) Akiyama, M.; Morofuji, Y.; Kamohara, T.; Nishikubo, K.; Tsubai, M.; Fukuda, O.; Ueno, N. Flexible Piezoelectric Pressure Sensors Using Oriented Aluminum Nitride Thin Films Prepared on Polyethylene Terephthalate Films. *J. Appl. Phys.* **2006**, *100*, 114318.
(34) Lee, C.-T.; Chiu, Y.-S. Piezoelectric ZnO-Nanorod-Structured Pressure Sensors Using GaN-Based Field-Effect-Transistor. *Appl. Phys. Lett.* **2015**, *106*, No. 073502.
(35) Graz, I.; Krause, M.; Bauer-Gogonea, S.; Bauer, S.; Lacour, S. P.; Ploss, B.; Zirkl, M.; Stadlober, B.; Wagner, S. Flexible Active-Matrix Cells with Selectively Poled Bifunctional Polymer-Ceramic Nanocomposite for Pressure and Temperature Sensing Skin. *J. Appl. Phys.* **2009**, *106*, No. 034503.
(36) Lin, L.; Xie, Y.; Wang, S.; Wu, W.; Niu, S.; Wen, X.; Wang, Z. L. Triboelectric Active Sensor Array for Self-Powered Static and Dynamic Pressure Detection and Tactile Imaging. *ACS Nano* **2013**, *7*, 8266−8274.
(37) Khan, Y.; Ostfeld, A. E.; Lochner, C. M.; Pierre, A.; Arias, A. C. Monitoring of Vital Signs with Flexible and Wearable Medical Devices. *Adv. Mater.* **2016**, *28*, 4373−4395.
(38) Boutry, C. M.; Nguyen, A.; Lawal, Q. O.; Chortos, A.; Rondeau-Gagné, S.; Bao, Z. A Sensitive and Biodegradable Pressure Sensor Array for Cardiovascular Monitoring. *Adv. Mater.* **2015**, *27*, 6954−6961.
(39) Kwon, D.; Lee, T.-I.; Shim, J.; Ryu, S.; Kim, M. S.; Kim, S.; Kim, T.-S.; Park, I. Highly Sensitive, Flexible, and Wearable Pressure Sensor Based on a Giant Piezocapacitive Effect of Three-Dimensional Microporous Elastomeric Dielectric Layer. *ACS Appl. Mater. Interfaces* **2016**, *8*, 16922−16931.
(40) Nie, B.; Li, R.; Cao, J.; Brandt, J. D.; Pan, T. Flexible Transparent Iontronic Film for Interfacial Capacitive Pressure Sensing. *Adv. Mater.* **2015**, *27*, 6055−6062.
(41) Mannsfeld, S. C. B.; Tee, B. C.-K.; Stoltenberg, R. M.; Chen, C. V. H.-H.; Barman, S.; Muir, B. V. O.; Sokolov, A. N.; Reese, C.; Bao, Z. Highly Sensitive Flexible Pressure Sensors with Microstructured Rubber Dielectric Layers. *Nat. Mater.* **2010**, *9*, 859−864.
(42) Schwartz, G.; Tee, B. C.-K.; Mei, J.; Appleton, A. L.; Kim, D. H.; Wang, H.; Bao, Z. Flexible Polymer Transistors with High Pressure Sensitivity for Application in Electronic Skin and Health Monitoring. *Nat. Commun.* **2013**, *4*, 1859.
(43) Sekitani, T.; Zschieschang, U.; Klauk, H.; Someya, T. Flexible Organic Transistors and Circuits with Extreme Bending Stability. *Nat. Mater.* **2010**, *9*, 1015−1022.
(44) Gong, S.; Schwalb, W.; Wang, Y.; Chen, Y.; Tang, Y.; Si, J.; Shirinzadeh, B.; Cheng, W. A Wearable and Highly Sensitive Pressure Sensor with Ultrathin Gold Nanowires. *Nat. Commun.* **2014**, *5*, 3132.
(45) Wang, X.; Gu, Y.; Xiong, Z.; Cui, Z.; Zhang, T. Silk-Molded Flexible, Ultrasensitive, and Highly Stable Electronic Skin for Monitoring Human Physiological Signals. *Adv. Mater.* **2014**, *26*, 1336−1342.
(46) Lee, B.-Y.; Kim, J.; Kim, H.; Kim, C.; Lee, S.-D. Low-Cost Flexible Pressure Sensor Based on Dielectric Elastomer Film with Micro-Pores. *Sens. Actuators, A* **2016**, *240*, 103−109.
(47) Jang, Y.; Jo, J.; Woo, K.; Lee, S.-H.; Kwon, S.; Kim, H.; Lee, H. S. Fabrication of Highly Sensitive Piezocapacitive Pressure Sensors Using a Simple and Inexpensive Home Milk Frother. *Phys. Rev. Appl.* **2019**, *11*, No. 014037.

https://dx.doi.org/10.1021/acsomega.0c02278
ACS Omega 2020, 5, 16944−16950